

The International Journal of Robotics Research

<http://ijr.sagepub.com/>

Hand-Eye Calibration Using Dual Quaternions

Konstantinos Daniilidis

The International Journal of Robotics Research 1999 18: 286

DOI: 10.1177/02783649922066213

The online version of this article can be found at:

<http://ijr.sagepub.com/content/18/3/286>

Published by:



<http://www.sagepublications.com>

On behalf of:



Multimedia Archives

Additional services and information for *The International Journal of Robotics Research* can be found at:

Email Alerts: <http://ijr.sagepub.com/cgi/alerts>

Subscriptions: <http://ijr.sagepub.com/subscriptions>

Reprints: <http://www.sagepub.com/journalsReprints.nav>

Permissions: <http://www.sagepub.com/journalsPermissions.nav>

Citations: <http://ijr.sagepub.com/content/18/3/286.refs.html>

>> [Version of Record](#) - Mar 1, 1999

[What is This?](#)

Konstantinos Daniilidis

GRASP Laboratory
University of Pennsylvania
Philadelphia, Pennsylvania 19104-6228, USA
kostas@grip.cis.upenn.edu

Hand-Eye Calibration Using Dual Quaternions

Abstract

To relate measurements made by a sensor mounted on a mechanical link to the robot's coordinate frame, we must first estimate the transformation between these two frames. Many algorithms have been proposed for this so-called hand-eye calibration, but they do not treat the relative position and orientation in a unified way. In this paper, we introduce the use of dual quaternions, which are the algebraic counterpart of screws. Then we show how a line transformation can be written with the dual-quaternion product. We algebraically prove that if we consider the camera and motor transformations as screws, then only the line coefficients of the screw axes are relevant regarding the hand-eye calibration. The dual-quaternion parameterization facilitates a new simultaneous solution for the hand-eye rotation and translation using the singular value decomposition. Real-world performance is assessed directly in the application of hand-eye information for stereo reconstruction, as well as in the positioning of cameras. Both real and synthetic experiments show the superiority of the approach over two other proposed methods.

1. Introduction

Hand-eye calibration is the computation of the relative position and orientation between the robot gripper and a camera mounted rigidly on the gripper. This problem also concerns all sensors that are rigidly mounted on mechanical links, such as a camera mounted on a binocular head with mechanical degrees of freedom, as well as a camera mounted on a vehicle. Although the term “sensor-actuator calibration” is actually more appropriate, throughout this paper we will use the more well-known term “hand-eye calibration.”

The hand-eye transformation is required in a number of sensing-acting tasks. Using a camera mounted on a gripper or a vehicle, we can estimate the position of a target to grasp or to reach in camera coordinates. However, the control commands can be expressed only in the coordinate system of the gripper or the vehicle. Even if the desired control criterion is given in camera coordinates, we have to know which is the effect of a robot motion in the camera frame.

The second task group is the placement of sensors at desired positions. We can achieve stereo reconstruction by placing a camera mounted on a gripper at multiple poses sharing the same field of view. However, to reconstruct the 3-D positions, we must know the relative orientation from the camera coordinate systems. But the only transformations we know are in the robot coordinates. The same applies for mounting cameras on binocular heads. As the cameras are manually mounted, a hand-eye calibration is necessary to align the camera coordinate system with the tilt-vergence link.

The usual way to describe the hand-eye calibration is by means of homogeneous transformation matrices. We denote¹ by X the transformation from camera to gripper, by A_i the transformation matrix from the camera to the world coordinate system, and by B_i the transformation matrix from the robot base to the gripper at the i th pose. Figure 1 illustrates one of the applications of hand-eye calibration, which consists of a camera mounted on a gripper. The camera-world transformation A_i is obtained with the extrinsic calibration techniques. The robot-base-to-gripper transformation B_i is given by the direct kinematic chain from the joint-angle readings. We see that for one pose we have two transformations as unknowns: robot-base-to-world, and the camera-to-gripper X . To eliminate the base-to-world transformation, we need one motion (two poses) that yields the well-known hand-eye equation first formulated by Shiu and Ahmad (1989) and Tsai and Lenz (1989),

$$AX = XB, \quad (1)$$

where $A = A_2A_1^{-1}$ and $B = B_2^{-1}B_1$. As every homogeneous transformation matrix has the form

$$\begin{pmatrix} R & \vec{t} \\ 0^T & 1 \end{pmatrix},$$

1. We use boldface capital letters for matrices X , arrowed boldface letters for 3-D vectors \vec{x} , boldface letters for real quaternions x , checked italicized fonts \check{x} for dual scalars, checked arrowed boldface for dual vectors $\check{\vec{x}}$, and checked italicized boldface for dual quaternions $\check{\check{x}}$. The natural inner product of two vectors or quaternions is denoted by $\vec{x}^T \vec{y}$, and the cross-product between 3-D vectors by $\vec{x} \times \vec{y}$.

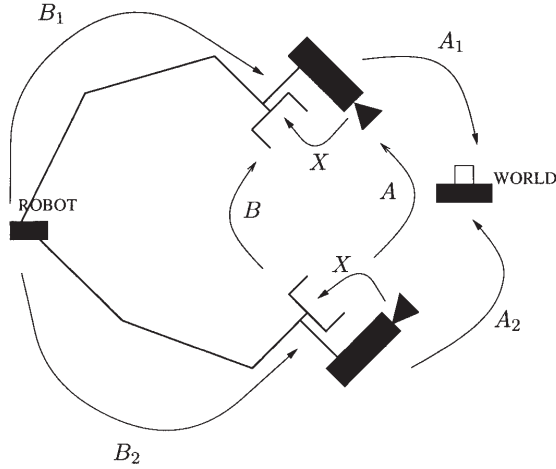


Fig. 1. The transformations between different frames at pose 1 and pose 2.

from eq. (1) follows one matrix and one vector equation

$$\mathbf{R}_A \mathbf{R}_X = \mathbf{R}_X \mathbf{R}_B, \quad (2)$$

$$(\mathbf{R}_A - \mathbf{I})\tilde{\mathbf{t}}_X = \mathbf{R}_X \tilde{\mathbf{t}}_B - \tilde{\mathbf{t}}_A. \quad (3)$$

The majority of the approaches regards the rotation estimation in eq. (2) decoupled from the translation estimation, the latter following the former. At least two rotations containing motions with nonparallel rotation axes are required to solve the problem (Tsai and Lenz 1989). Several approaches have been proposed for the estimation of \mathbf{R}_X from eq (2): using the rotation axis and angle (Tsai and Lenz 1989; Shiu and Ahmad 1989), quaternions (Chou and Kamel 1991), and canonical matrix representation (Li and Betsis 1995) (a survey is provided by Wang 1992).

Horaud and Dornaika (1995) emphasize the fact that the computation of the extrinsic calibration matrices \mathbf{A}_i given the projection matrices \mathbf{M}_i from world to pixel coordinates is an unstable problem. Therefore, they propose the following alternative: assume that the matrix of intrinsic parameters \mathbf{C} remains constant during motion. Then the projection matrix reads

$$\mathbf{M}_i = \mathbf{C} \mathbf{A}_i = \begin{pmatrix} \mathbf{C} \mathbf{R}_{A_i} & \mathbf{C} \tilde{\mathbf{t}}_{A_i} \end{pmatrix}. \quad (4)$$

We introduce $\mathbf{N}_i = \mathbf{C} \mathbf{R}_{A_i}$ and $\tilde{\mathbf{n}}_i = \mathbf{C} \tilde{\mathbf{t}}_{A_i}$. Let us assume that one extrinsic calibration \mathbf{A}_1 is known, and replace $\mathbf{X} = \mathbf{A}_1 \mathbf{Y}$. The unknown is now the world-gripper transformation \mathbf{Y} . Equation (1) can be rewritten as

$$\mathbf{A}_2 \mathbf{Y} = \mathbf{A}_1 \mathbf{Y} \mathbf{B} \quad \text{or} \quad \mathbf{A}_1^{-1} \mathbf{A}_2 \mathbf{Y} = \mathbf{Y} \mathbf{B}, \quad (5)$$

which is just a new homogeneous transform equation. However, if we write $\mathbf{A}_1^{-1} \mathbf{A}_2$ as a function of the projection parameters, we find that $\mathbf{A}_1^{-1} \mathbf{A}_2$ is independent of the intrinsic parameters \mathbf{C} :

$$\mathbf{A}_1^{-1} \mathbf{A}_2 = \begin{pmatrix} \mathbf{N}_1^{-1} \mathbf{N}_2 & \mathbf{N}_1^{-1} (\tilde{\mathbf{n}}_2 - \tilde{\mathbf{n}}_1) \\ \mathbf{0}^T & 1 \end{pmatrix}. \quad (6)$$

Hence, with an appropriate change of the unknown, we obtain eq. (5) which can be solved by all the methods solving eq. (1) as well as the one proposed later in this paper.

Horaud and Dornaika (1995) were the first to apply a simultaneous nonlinear minimization with respect to the rotation quaternion and the translation vector. However, the first simultaneous consideration of rotation and translation in a geometric way was presented by Chen (1991), who first introduced the screw theory in the hand-eye calibration.

In this paper, we introduce the algebraic entity for a screw: the unit dual quaternion. Dual quaternions are an extension of the real quaternions by means of the dual numbers (Study 1891; Blaschke 1960), and were first introduced by Clifford (1873). Dual numbers and dual quaternions were used earlier in robotics (Walker 1988; Gu and Luh 1987; Funda and Paul 1990), and in computer vision (Walker, Shao, and Volz 1991; Phong et al. 1993). Based on the dual quaternions, we prove that:

1. the hand-eye transformation is independent of the angle and the pitch of the camera and hand motions, and depends only on the line parameters of their screw axes—a result geometrically proved by Chen (1991); and
2. the unknown screw parameters, including both rotation and translation, can be simultaneously recovered using the singular value decomposition (SVD).

This is the first algorithm in the literature simultaneously solving for rotation and translation without nonlinear minimization. The algorithm was implemented and compared with a two-step algorithm that separately solves for \mathbf{R} and $\tilde{\mathbf{t}}$, showing its superior performance. The performance with real data is tested directly in an application. We judge the quality of the obtained hand-eye information on the task of stereo reconstruction using the motor-encoder readings of an active camera.

The next section gives an exposition on the properties of dual numbers and dual quaternions. Then, we describe how a line transformation is expressed with dual quaternions, and how we obtain a dual quaternion from the $(\mathbf{R}, \tilde{\mathbf{t}})$ representation. The dual quaternion is given as a function of the screw parameters, and then we prove the independence result. We describe our solution via SVD, and end with experimental results.

2. Dual Quaternions

This section outlines briefly the dual quaternions. First quaternions are explained, followed by a short description of dual numbers. Finally, the dual quaternions and their relevant properties are introduced.

2.1. Quaternions

Invented by Hamilton (Blaschke 1960), quaternions are an extension of the complex numbers to \mathcal{R}^4 . Among other formalisms, one definition of quaternions is as pairs (s, \vec{q}) , where $s \in \mathcal{R}$ and $\vec{q} \in \mathcal{R}^3$. The following operations

$$\mathbf{q}_1 + \mathbf{q}_2 = (s_1 + s_2, \vec{q}_1 + \vec{q}_2), \quad (7)$$

$$\lambda(s, \vec{q}) = (\lambda s, \lambda \vec{q}), \quad (8)$$

where $\lambda \in \mathcal{R}$ make the quaternions a vector space over the reals—we will call \mathcal{H} —with the zero element $(0, \mathbf{0})$. The multiplication between quaternions, which is defined as

$$\mathbf{q}_1 \mathbf{q}_2 = (s_1 s_2 - \vec{q}_1^T \vec{q}_2, s_1 \vec{q}_2 + s_2 \vec{q}_1 + \vec{q}_1 \times \vec{q}_2), \quad (9)$$

has a unit element $(1, \mathbf{0})$, and is associative but not commutative. Therefore, the quaternions are an associative algebra, and since they do not contain zero divisors, they are a division algebra. The norm of a quaternion is defined as $\|\mathbf{q}\| = \mathbf{q} \bar{\mathbf{q}}$, where $\bar{\mathbf{q}}$ is the conjugate quaternion $(s, -\vec{q})$. A subgroup of \mathcal{H} regarding only the multiplication operation includes the unit quaternions with norm equal one. For every rotation (element of $\text{SO}(3)$) about an axis \vec{n} ($\|\vec{n}\| = 1$) with an angle θ , a corresponding unit quaternion $\mathbf{q} = (\cos \frac{\theta}{2}, \sin \frac{\theta}{2} \vec{n})$ exists that maps a vector $\vec{x} \in \mathcal{R}^3$ to the vector $\mathbf{q}(0, \vec{x})\bar{\mathbf{q}}$.

2.2. Dual Numbers

Dual numbers were invented by Clifford (1873), and further developed by Study (1891) in the last century. A dual number is defined as

$$\check{z} = a + \epsilon b \quad \text{with} \quad \epsilon^2 = 0. \quad (10)$$

The operations addition and multiplication make them an Abelian ring called Δ , but not a field, because only dual numbers with real part not zero possess an inverse element. An important property is associated with the derivatives of functions with dual arguments. Since all powers of ϵ greater than one vanish, a Taylor expansion yields

$$f(a + \epsilon b) = f(a) + \epsilon b f'(a). \quad (11)$$

Dual vectors are defined in Δ^3 ; with the addition and the external multiplication with a dual number, they make a module over the ring Δ . Dual vectors with orthogonal real and dual parts are a representation of lines in \mathcal{R}^3 known as Plücker coordinates. The real part is the direction of the line, and the dual part is its moment. The inner product between two such dual vectors is equal to the cosine of a dual angle $\check{\theta} = \theta + \epsilon d$, which has a nice geometric interpretation: θ is the angle between the two space lines, and d is their distance.

2.3. Dual Quaternions

Dual quaternions are defined in a similar way to real quaternions as $(\check{s}, \check{\vec{q}})$ where \check{s} is a dual number and $\check{\vec{q}}$ is a dual vector. The operations have the same definitions:

$$\check{\mathbf{q}}_1 + \check{\mathbf{q}}_2 = (\check{s}_1 + \check{s}_2, \check{\vec{q}}_1 + \check{\vec{q}}_2), \quad (12)$$

$$\check{\lambda}(\check{s}, \check{\vec{q}}) = (\check{\lambda}\check{s}, \check{\lambda}\check{\vec{q}}), \quad (13)$$

$$\check{\mathbf{q}}_1 \check{\mathbf{q}}_2 = (\check{s}_1 \check{s}_2 - \check{\vec{q}}_1^T \check{\vec{q}}_2, \check{s}_1 \check{\vec{q}}_2 + \check{s}_2 \check{\vec{q}}_1 + \check{\vec{q}}_1 \times \check{\vec{q}}_2). \quad (14)$$

The first two, eqs. (12) and (13), make the dual quaternions a Δ -module. Addition (12) and multiplication (14) make them a non-Abelian ring with unit element $(1, \mathbf{0})$. All three operations make them an associative algebra. Dual vectors $\check{\vec{q}}$ can be written as dual quaternions $(0, \check{\vec{q}})$, and their multiplication possesses the nice property

$$(0, \check{\vec{q}}_1)(0, \check{\vec{q}}_2) = (-\check{\vec{q}}_1^T \check{\vec{q}}_2, \check{\vec{q}}_1 \times \check{\vec{q}}_2). \quad (15)$$

The norm of a dual quaternion is defined as $\|\check{\mathbf{q}}\|^2 = \check{\mathbf{q}} \check{\bar{\mathbf{q}}}$, and is a dual number with a positive real part. If the norm has a nonvanishing real part, then the dual quaternion has an inverse $\check{\mathbf{q}}^{-1} = \|\check{\mathbf{q}}\|^{-1} \check{\bar{\mathbf{q}}}$. If the norm is equal to one, then an inverse element exists and is equal to the conjugate quaternion. If $\check{\mathbf{q}} = \mathbf{q} + \epsilon \mathbf{q}'$, then the unity condition $\check{\mathbf{q}} \check{\bar{\mathbf{q}}} = 1$ can be written

$$\mathbf{q} \bar{\mathbf{q}} = 1 \quad \text{and} \quad \bar{\mathbf{q}} \mathbf{q}' + \bar{\mathbf{q}}' \mathbf{q} = 0. \quad (16)$$

As we shall describe in the following unit, dual quaternions represent general motions of lines and the expression $\check{\mathbf{q}} \check{\mathbf{x}} \check{\bar{\mathbf{q}}}$ that is valid for the rotation of points in the case of real quaternions is also true for the general motion of lines in the case of dual quaternions.

3. Line Transformations with Unit Dual Quaternions

As is already known, the rotation of a point \vec{p}_b to a point \vec{p}_a can be written by means of a unit quaternion \mathbf{q} , as the product $\vec{p}_a = \mathbf{q} \vec{p}_b \bar{\mathbf{q}}$. This form allows the concatenation of rotations to be represented by a simple quaternion product. Unfortunately, no such quaternion representation exists for a general rigid transformation that includes translation. We will explain in this section that the introduction of dual quaternions allows a rigid-transformation rule as simple as the one for pure rotations; however, not for a point but for a line.

A line in space with direction \vec{l} through a point \vec{p} can be represented with the six-tuple (\vec{l}, \vec{m}) , where \vec{m} is called the line moment and is equal to $\vec{p} \times \vec{l}$. The line moment is normal to the plane through the line and the origin, with magnitude equal to the distance from the line to the origin. The constraints $\|\vec{l}\| = 1$ and $\vec{l}^T \vec{m} = 0$ guarantee that the degrees of freedom of an arbitrary line in space are four.

We next give an answer to the following problem.

PROBLEM 1. A line given by its dual quaternion $\check{l}_a = l_a + \epsilon m_a$ is transformed with (R, \vec{t}) into a line \check{l}_b . Show that a unit dual quaternion exists such that $\check{l}_a = \check{q} \check{l}_b \check{q}$.

Applying a rotation R and a translation \vec{t} to a line (\vec{l}_b, \vec{m}_b) , we obtain the transformed line (\vec{l}_a, \vec{m}_a) :

$$\vec{l}_a = R\vec{l}_b, \quad (17)$$

$$\begin{aligned} \vec{m}_a &= \vec{p}_a \times \vec{l}_a = (R\vec{p}_b + \vec{t}) \times R\vec{l}_b, \\ &= R(\vec{p}_b \times \vec{l}_b) + \vec{t} \times R\vec{l}_b, \\ &= R\vec{m}_b + \vec{t} \times R\vec{l}_b. \end{aligned} \quad (18)$$

We change from vector to quaternion notation, which means that the vector \vec{l} is represented by a quaternion with zero scalar part $l = (0, \vec{l})$. The terms containing rotation can be easily written with quaternions. The difficulty with the cross-product is tackled with the identity

$$(0, \vec{t} \times \vec{q}) = \frac{1}{2}(q\vec{t} + t\vec{q}), \quad (19)$$

where t is the translation quaternion $(0, \vec{t})$, and q is the rotation quaternion $(0, \vec{q})$. Using the identity eq. (19), we obtain

$$\begin{aligned} l_a &= ql_b\bar{q}, \\ m_a &= qm_b\bar{q} + \frac{1}{2}(ql_b\bar{q}\vec{t} + tql_b\bar{q}). \end{aligned} \quad (20)$$

We define a new quaternion $q' = \frac{1}{2}tq$ and a dual quaternion $\check{q} = q + \epsilon q'$. It can be easily shown that eq. (20) is equivalent to

$$l_a + \epsilon m_a = (q + \epsilon q')(l_b + \epsilon m_b)(\bar{q} + \epsilon \bar{q}'). \quad (21)$$

Denoting also the lines by dual quaternions \check{l}_a and \check{l}_b , we obtain

$$\check{l}_a = \check{q} \check{l}_b \check{q}.$$

This formula resembles the rotation of points with quaternions.

Lines can thus be rigidly transformed using a single operation (multiplying left and right sides with the conjugate) in the non-Abelian ring of dual quaternions. The norm

$$\begin{aligned} |\check{q}|^2 &= \check{q}\bar{\check{q}} = q\bar{q} + \epsilon(q\bar{q}' + q'\bar{q}) \\ &= q\bar{q} + \epsilon/2(q\bar{q}\vec{t} + t\bar{q}\bar{q}) = 1, \end{aligned}$$

hence \check{q} is a unit dual quaternion. The above relations also explicitly give the transformation from (R, \vec{t}) to $q + \epsilon q'$. The dual part $q' = \frac{1}{2}tq$ and the quaternion q can be obtained from the rotation matrix by finding the axis and the angle of rotation. If \check{q} is a solution, then $-\check{q}$ is also a solution. As in

nondual quaternions, it is sufficient to enforce that the scalar nondual part be positive to eliminate this ambiguity.

Conversely, the translation t can be recovered from the dual quaternion as

$$t = 2q'\bar{q}. \quad (22)$$

The unit dual quaternion \check{q} can be written as the concatenation of a pure translational unit dual quaternion and a pure rotational quaternion with dual part equal to zero; i.e.,

$$\check{q} = (1, \epsilon \frac{\vec{t}}{2})q.$$

4. Unit Dual Quaternions and Screws

This section shows that the scalar and the vector parts of the dual quaternion have specific meanings which relate them to the kinematic notion of a screw. According to Chasles's theorem (Chen 1991), a rigid transformation can be modeled as a rotation *with the same angle* about an axis not through the origin and a translation along this axis. As the screw axis is a line in space, it depends on four parameters which together with the rotation angle θ and the translation along the d (pitch) axis constitute the six degrees of freedom of a rigid transformation.

We solve the following problem.

PROBLEM 2. Given a rotation R about an axis through the origin and a translation \vec{t} , compute the pitch d as well as the screw axis given by its direction and moment pair (\vec{l}, \vec{m}) .

The direction \vec{l} is parallel to the rotation axis. The pitch d is the projection of translation on the rotation axis, and is therefore equal to $\vec{t}^T \vec{l}$. The not-mentioned angle, θ , is the same in both the (R, \vec{t}) and the screw representation. To recover the moment \vec{m} , we introduce a point \vec{c} on the screw axis as the projection of the origin on the axis (Fig. 2).

The coordinate system is shifted to this point and then transformed. The resulting translation is then $d\vec{l} + (I - R)\vec{c}$.

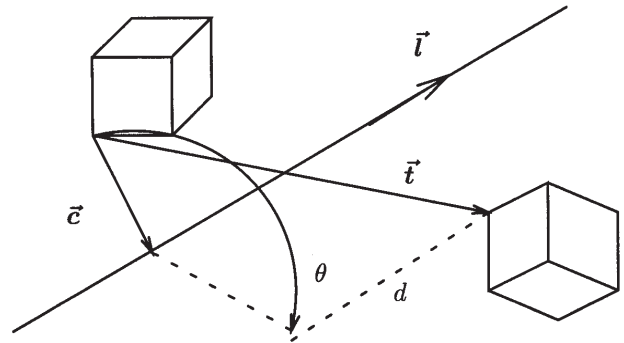


Fig. 2. The geometry of a screw: every motion can be modeled as a rotation with angle θ about an axis at \vec{c} , with direction \vec{l} and a subsequent translation d along the axis.

The so-called pitch d reads $d = \tilde{\mathbf{l}}^T \tilde{\mathbf{t}}$. Using the Rodrigues formula,

$$\mathbf{R}\tilde{\mathbf{c}} = \tilde{\mathbf{c}} + \sin(\theta)\tilde{\mathbf{l}} \times \tilde{\mathbf{c}} + (1 - \cos \theta)\tilde{\mathbf{l}} \times (\tilde{\mathbf{l}} \times \tilde{\mathbf{c}}),$$

and $\tilde{\mathbf{c}}^T \tilde{\mathbf{l}} = 0$, it follows that

$$\tilde{\mathbf{c}} = \frac{1}{2}(\tilde{\mathbf{t}} - (\tilde{\mathbf{t}}^T \tilde{\mathbf{l}})\tilde{\mathbf{l}}) + \cot \frac{\theta}{2} \tilde{\mathbf{l}} \times \tilde{\mathbf{t}}. \quad (23)$$

This point $\tilde{\mathbf{c}}$ and hence the screw axis is not defined if the angle θ is either 0 or 180°. Otherwise the moment vector then reads

$$\tilde{\mathbf{m}} = \tilde{\mathbf{c}} \times \tilde{\mathbf{l}} = \frac{1}{2}(\tilde{\mathbf{t}} \times \tilde{\mathbf{l}} + \tilde{\mathbf{l}} \times (\tilde{\mathbf{t}} \times \tilde{\mathbf{l}}) \cot \frac{\theta}{2}). \quad (24)$$

We proceed with the computation of the corresponding quaternion: given the screw parameters $(\theta, d, \tilde{\mathbf{l}}, \tilde{\mathbf{m}})$, compute the corresponding dual quaternion $\check{\mathbf{q}}$.

The quaternion derived from the rotation matrix \mathbf{R} reads

$$(q_0, \tilde{\mathbf{q}}) = (\cos \frac{\theta}{2}, \sin \frac{\theta}{2} \tilde{\mathbf{l}}), \quad (25)$$

hence the moment eq. (24) can be written

$$\sin \frac{\theta}{2} \tilde{\mathbf{m}} = \frac{1}{2}(\tilde{\mathbf{t}} \times \tilde{\mathbf{q}} + q_0 \tilde{\mathbf{t}} - \cos \frac{\theta}{2} (\tilde{\mathbf{l}}^T \tilde{\mathbf{t}}) \tilde{\mathbf{l}}).$$

Using $(\tilde{\mathbf{l}}^T \tilde{\mathbf{t}}) = d$ and rewriting

$$\sin \frac{\theta}{2} \tilde{\mathbf{m}} + \frac{d}{2} \cos \frac{\theta}{2} \tilde{\mathbf{l}} = \frac{1}{2}(\tilde{\mathbf{t}} \times \tilde{\mathbf{q}} + q_0 \tilde{\mathbf{t}})$$

(which is the vector part of the dual part \mathbf{q}' of the dual quaternion $\check{\mathbf{q}}$), applying eq. (25), and using $\mathbf{q}' = \frac{1}{2} \mathbf{t} \mathbf{q}$, we obtain

$$\begin{aligned} \check{\mathbf{q}} &= \begin{pmatrix} q_0 \\ \tilde{\mathbf{q}} \end{pmatrix} + \epsilon \begin{pmatrix} -\frac{1}{2} \tilde{\mathbf{q}}^T \tilde{\mathbf{t}} \\ \frac{1}{2} (q_0 \tilde{\mathbf{t}} + \tilde{\mathbf{t}} \times \tilde{\mathbf{q}}) \end{pmatrix} = \begin{pmatrix} \cos \frac{\theta}{2} \\ \sin \frac{\theta}{2} \tilde{\mathbf{l}} \end{pmatrix} \\ &+ \epsilon \begin{pmatrix} -\frac{d}{2} \sin \frac{\theta}{2} \\ \sin \frac{\theta}{2} \tilde{\mathbf{m}} + \frac{d}{2} \cos \frac{\theta}{2} \tilde{\mathbf{l}} \end{pmatrix}. \end{aligned} \quad (26)$$

Every function f of the dual numbers obeys the rule

$$f(a + \epsilon b) = f(a) + \epsilon b f'(a),$$

hence

$$\cos\left(\frac{\theta + \epsilon d}{2}\right) = \cos \frac{\theta}{2} - \epsilon \frac{d}{2} \sin \frac{\theta}{2},$$

and

$$\sin\left(\frac{\theta + \epsilon d}{2}\right) = \sin \frac{\theta}{2} + \epsilon \frac{d}{2} \cos \frac{\theta}{2}.$$

It is now straightforward to see that a dual quaternion can also be written as

$$\check{\mathbf{q}} = \begin{pmatrix} \cos\left(\frac{\theta + \epsilon d}{2}\right) \\ \sin\left(\frac{\theta + \epsilon d}{2}\right)(\tilde{\mathbf{l}} + \epsilon \tilde{\mathbf{m}}) \end{pmatrix}. \quad (27)$$

This representation is very powerful since it algebraically separates the angle and pitch information from the line information characterizing the pose of the screw axis. Moreover, writing the dual angle $\check{\theta} = \theta + \epsilon d$ and the dual vector $\check{\tilde{\mathbf{l}}} = \tilde{\mathbf{l}} + \epsilon \tilde{\mathbf{m}}$, eq. (27) becomes equivalent to the pure rotation of the nondual eq. (25). We can easily verify that

$$\check{\mathbf{q}} = (\cos \check{\theta}/2, \check{\tilde{\mathbf{l}}} \sin \check{\theta}/2)$$

is a unit quaternion $\check{\mathbf{q}}\check{\mathbf{q}} = 1$.

5. Hand-Eye Transformation with Unit Dual Quaternions

The concatenation of two rigid displacements or screws can be written as the product of two dual quaternions. Let $\check{\mathbf{a}}$ denote the screw of a camera motion, and $\check{\mathbf{b}}$ denote the screw of the motor motion. Motor (hand) and camera (eye) are rigidly attached to each other. The rigid transformation between them is unknown, and it will be denoted by the unit dual quaternion $\check{\mathbf{q}}$. The screw concatenation then yields

$$\check{\mathbf{a}} = \check{\mathbf{q}}\check{\mathbf{b}}\check{\mathbf{q}}, \quad (28)$$

which is the most compact equation for the hand-eye relationship since the dual quaternion components are 8 and not 12 like in the homogeneous matrices of eq. (1). The scalar part of a dual quaternion $\check{\mathbf{a}}$ is $(\check{\mathbf{a}} + \check{\tilde{\mathbf{a}}})/2$, hence

$$\begin{aligned} Sc(\check{\mathbf{a}}) &= \frac{1}{2}(\check{\mathbf{a}} + \check{\tilde{\mathbf{a}}}) = \frac{1}{2}(\check{\mathbf{q}}\check{\mathbf{b}}\check{\mathbf{q}} + \check{\mathbf{q}}\check{\tilde{\mathbf{b}}}\check{\mathbf{q}}) = \frac{1}{2}\check{\mathbf{q}}(\check{\mathbf{b}} + \check{\tilde{\mathbf{b}}})\check{\mathbf{q}} \\ &= \check{\mathbf{q}}Sc(\check{\mathbf{b}})\check{\mathbf{q}} = Sc(\check{\mathbf{b}})\check{\mathbf{q}}\check{\mathbf{q}} = Sc(\check{\mathbf{b}}). \end{aligned} \quad (29)$$

According to eq. (27), the scalar parts are equal to the cosine of the respective dual angles:

$$\cos \frac{(\theta_a + \epsilon d_a)}{2} = \cos \frac{(\theta_b + \epsilon d_b)}{2},$$

which is equivalent to

$$\cos \frac{\theta_a}{2} = \cos \frac{\theta_b}{2} \quad \text{and} \quad d_a \sin \frac{\theta_a}{2} = d_b \sin \frac{\theta_b}{2}.$$

Hence, the angle and the pitch of the motor screw are equal to the angle and the pitch of the camera screw; therefore the angle and the pitch remain invariant under coordinate transformations. This is also known as the screw congruence theorem (Chen 1991), its proof without dual unit quaternions is, however, considerably longer than the one-line proof in eq. (29).

The fundamental equation $\check{\mathbf{a}} = \check{\mathbf{q}}\check{\mathbf{b}}\check{\mathbf{q}}$ consists of four dual equations. Since the scalar parts are equal, only the vector components contribute to the computation of the unknown $\check{\mathbf{q}}$:

$$\sin \frac{\theta_a}{2} (0, \check{\mathbf{a}}) = \check{\mathbf{q}} (0, \sin \frac{\theta_b}{2} \check{\mathbf{b}}) \check{\mathbf{q}} = \sin \frac{\theta_b}{2} \check{\mathbf{q}} (0, \check{\mathbf{b}}) \check{\mathbf{q}}.$$

If the angles $\theta_{a,b}$ are not 0 or 360° , the sines can be simplified, yielding

$$(0, \check{\mathbf{a}}) = \check{\mathbf{q}} (0, \check{\mathbf{b}}) \check{\mathbf{q}}, \quad (30)$$

which is nothing other than the motion of the lines of the screw axes.

Thus,

1. the hand-eye estimation is independent of the angle and the pitch of the camera and the motor motions, and
2. the hand-eye calibration is equivalent to the 3-D motion-estimation problem from 3-D line correspondences, where the lines are the screw axes of the motors and the cameras.

We should note here that all other hand-eye calibration methods make use of the rotation angle and the pitch, at least at the translation-estimation step of eq. (3), which turns out in eq. (30) to be unnecessary. Having shown that the problem is equivalent to the 3-D motion problem, we already know from computer vision (Sabata and Aggarwal 1991) that the minimum requirement is two nonparallel lines. Hence, the minimal data for hand-eye calibration are two motions with nonparallel rotation axes.

6. Estimation of the Hand-Eye Screw with SVD

Although we showed in the last section that only the vector part of the dual quaternions is relevant for the estimation of the unknown hand-eye unit dual quaternion $\check{\mathbf{q}}$, let us keep the same notation $\check{\mathbf{a}}$ and $\check{\mathbf{b}}$ for $(0, \check{\mathbf{b}})$ and $(0, \check{\mathbf{a}})$, respectively.

We split the fundamental eq. (28) into the nondual and dual parts, and we obtain

$$\begin{aligned} \mathbf{a} &= \mathbf{q}\mathbf{b}\bar{\mathbf{q}} \\ \mathbf{a}' &= \mathbf{q}\mathbf{b}\bar{\mathbf{q}}' + \mathbf{q}\mathbf{b}'\bar{\mathbf{q}} + \mathbf{q}'\mathbf{b}\bar{\mathbf{q}}. \end{aligned}$$

Multiplying on the right with \mathbf{q} and applying the identity

$$\bar{\mathbf{q}}\mathbf{q}' + \bar{\mathbf{q}}'\mathbf{q} = 0$$

in the first term of the right-hand side of the first equation yields

$$\begin{aligned} \mathbf{a}\mathbf{q} &= \mathbf{q}\mathbf{b}, \\ \mathbf{a}'\mathbf{q} &= -\mathbf{a}\mathbf{q}' + \mathbf{q}\mathbf{b}' + \mathbf{q}'\mathbf{b}, \end{aligned}$$

which may be rewritten as

$$\begin{aligned} \mathbf{a}\mathbf{q} - \mathbf{q}\mathbf{b} &= 0, \\ (\mathbf{a}'\mathbf{q} - \mathbf{q}\mathbf{b}') + (\mathbf{a}\mathbf{q}' - \mathbf{q}'\mathbf{b}) &= 0. \end{aligned}$$

We keep in mind that from each of the two equations above the scalar part is redundant, because they are equivalent to eq. (30). Hence, we have in total six equations with eight unknowns, which can be written in matrix form as follows. Let $\mathbf{a} = (0, \check{\mathbf{a}})$ and $\mathbf{a}' = (0, \check{\mathbf{a}}')$, as well as $\mathbf{b} = (0, \check{\mathbf{b}})$ and $\mathbf{b}' = (0, \check{\mathbf{b}}')$. The quaternion equations above can then be written as a matrix vector equation

$$\begin{pmatrix} \bar{\mathbf{a}} - \bar{\mathbf{b}} & [\bar{\mathbf{a}} + \bar{\mathbf{b}}]_{\times} & \mathbf{0}_{3 \times 1} & \mathbf{0}_{3 \times 3} \\ \bar{\mathbf{a}}' - \bar{\mathbf{b}}' & [\bar{\mathbf{a}}' + \bar{\mathbf{b}}']_{\times} & \bar{\mathbf{a}} - \bar{\mathbf{b}} & [\bar{\mathbf{a}} + \bar{\mathbf{b}}]_{\times} \end{pmatrix} \begin{pmatrix} \mathbf{q} \\ \mathbf{q}' \end{pmatrix} = 0, \quad (31)$$

where the matrix—we will call it \mathbf{S} —is a 6×8 matrix, and the vector of unknowns $(\mathbf{q}^T, \mathbf{q}'^T)$ is 8-dimensional. We denote with $[\bar{\mathbf{a}}]_{\times}$ the antisymmetric matrix corresponding to the cross-product with $\bar{\mathbf{a}}$.

Recall that we have two constraints on the unknowns so that the result is a unit dual quaternion

$$\mathbf{q}^T \mathbf{q} = 1, \quad \text{and} \quad \mathbf{q}^T \mathbf{q}' = 0. \quad (32)$$

We could think that six equations plus two constraints would suffice; however, the vectors $\bar{\mathbf{a}}$ and $\bar{\mathbf{b}}$ are unit vectors and the vectors $\bar{\mathbf{a}}'$ and $\bar{\mathbf{b}}'$ are perpendicular to $\bar{\mathbf{a}}$ and $\bar{\mathbf{b}}$, so that two equations are redundant. This is nothing new, since it is well known that at least two lines are necessary so that 3-D motion can be estimated from their correspondences (Sabata and Aggarwal 1991). Thus, we need at least two motions of the hand-eye system to get two lines from the corresponding screws. Chen (1991) also recognized this fact, and analyzed the uniqueness of the problem. He geometrically proved that even in the case of two parallel rotation axes we can compute all parameters up to the pitch.

Suppose now that $n \geq 2$ motions are given. We construct the $6n \times 8$ matrix

$$\mathbf{T} = (\mathbf{S}_1^T \quad \mathbf{S}_2^T \quad \dots \quad \mathbf{S}_n^T)^T, \quad (33)$$

which in the noise-free case has rank 6. Since in the noise-free case the equations arise from natural constraints, the null space contains at least the solution $(\mathbf{q}, \mathbf{q}')$. It is trivial to see that an additional orthogonal solution is $(\mathbf{0}_{4 \times 1}, \mathbf{q})$. Hence, the matrix is maximally of rank 6. If all axes $\bar{\mathbf{b}}$ are mutually parallel, then the rank of the matrix is 5. The proof is quite lengthy and will not be given here; however, it is plausible that in this case a three-parameter family of solutions cannot be constrained by the two conditions of eq. (32).

We compute the singular value decomposition $\mathbf{T} = \mathbf{U}\mathbf{\Sigma}\mathbf{V}^T$, where $\mathbf{\Sigma}$ is a diagonal matrix with the singular values,

the columns of U are the left-singular vectors, and the columns of V are the right-singular vectors. If the rank is 6, then the last two right-singular vectors $\tilde{\mathbf{v}}_7$ and $\tilde{\mathbf{v}}_8$ —corresponding to the two vanishing singular values—span the null space of T . We write them as being composed of two 4×1 vectors, $\tilde{\mathbf{v}}_7^T = (\tilde{\mathbf{u}}_1^T, \tilde{\mathbf{v}}_1^T)$ and $\tilde{\mathbf{v}}_8^T = (\tilde{\mathbf{u}}_2^T, \tilde{\mathbf{v}}_2^T)$. A vector $(\mathbf{q}^T, \mathbf{q}'^T)$ satisfying $T(\mathbf{q}^T, \mathbf{q}'^T)^T = 0$ must be a linear combination of $\tilde{\mathbf{v}}_7$ and $\tilde{\mathbf{v}}_8$. Hence

$$\begin{pmatrix} \mathbf{q} \\ \mathbf{q}' \end{pmatrix} = \lambda_1 \begin{pmatrix} \tilde{\mathbf{u}}_1 \\ \tilde{\mathbf{v}}_1 \end{pmatrix} + \lambda_2 \begin{pmatrix} \tilde{\mathbf{u}}_2 \\ \tilde{\mathbf{v}}_2 \end{pmatrix}.$$

The two degrees of freedom are fixed by the constraints of eq. (32), which imply two quadratic equations in λ_1 and λ_2 :

$$\lambda_1^2 \tilde{\mathbf{u}}_1^T \tilde{\mathbf{u}}_1 + 2\lambda_1 \lambda_2 \tilde{\mathbf{u}}_1^T \tilde{\mathbf{u}}_2 + \lambda_2^2 \tilde{\mathbf{u}}_2^T \tilde{\mathbf{u}}_2 = 1, \quad (34)$$

$$\lambda_1^2 \tilde{\mathbf{u}}_1^T \tilde{\mathbf{v}}_1 + \lambda_1 \lambda_2 (\tilde{\mathbf{u}}_1^T \tilde{\mathbf{v}}_2 + \tilde{\mathbf{u}}_2^T \tilde{\mathbf{v}}_1) + \lambda_2^2 \tilde{\mathbf{u}}_2^T \tilde{\mathbf{v}}_2 = 0. \quad (35)$$

Since λ_1 and λ_2 never both vanish, assume without loss of generality that $\tilde{\mathbf{u}}_1^T \tilde{\mathbf{v}}_1 \neq 0$, so that $\lambda_2 \neq 0$. Setting $s = \lambda_1/\lambda_2$ we first solve eq. (35), obtaining two solutions for s . Inserting $\lambda_1 = s\lambda_2$ in eq. (34) yields

$$\lambda_2^2 (s^2 \tilde{\mathbf{u}}_1^T \tilde{\mathbf{u}}_1 + 2s \tilde{\mathbf{u}}_1^T \tilde{\mathbf{u}}_2 + \tilde{\mathbf{u}}_2^T \tilde{\mathbf{u}}_2) = 1, \quad (36)$$

which has two real solutions of opposite sign, because it can be easily proved that the trinomial

$$(s^2 \tilde{\mathbf{u}}_1^T \tilde{\mathbf{u}}_1 + 2s \tilde{\mathbf{u}}_1^T \tilde{\mathbf{u}}_2 + \tilde{\mathbf{u}}_2^T \tilde{\mathbf{u}}_2)$$

is always positive or zero. Indeed, the second-order coefficient $\tilde{\mathbf{u}}_1^T \tilde{\mathbf{u}}_1$ is positive, and the discriminant $4(\tilde{\mathbf{u}}_1^T \tilde{\mathbf{u}}_2)^2 - 4(\tilde{\mathbf{u}}_1^T \tilde{\mathbf{u}}_1)(\tilde{\mathbf{u}}_2^T \tilde{\mathbf{u}}_2)$ is always negative or equal to zero due to the Schwartz inequality. We can easily prove that in the noise-free case the discriminant is equal to zero and an s exists that makes the left side of eq. (36) vanish: if $(\mathbf{q}^T, \mathbf{q}'^T)$ is a solution, then $(\mathbf{0}_{4 \times 1}, \mathbf{q})$ belongs to the kernel of the matrix T . Hence, λ_1 and λ_2 exist so that $\lambda_1 \tilde{\mathbf{u}}_1 + \lambda_2 \tilde{\mathbf{u}}_2 = 0$: that means $\tilde{\mathbf{u}}_1$ and $\tilde{\mathbf{u}}_2$ are parallel and the discriminant $4(\tilde{\mathbf{u}}_1^T \tilde{\mathbf{u}}_2)^2 - 4(\tilde{\mathbf{u}}_1^T \tilde{\mathbf{u}}_1)(\tilde{\mathbf{u}}_2^T \tilde{\mathbf{u}}_2)$ vanishes. Then, the double solution of $s^2 \tilde{\mathbf{u}}_1^T \tilde{\mathbf{u}}_1 + 2s \tilde{\mathbf{u}}_1^T \tilde{\mathbf{u}}_2 + \tilde{\mathbf{u}}_2^T \tilde{\mathbf{u}}_2$ for s is $-\|\tilde{\mathbf{u}}_1\|/\|\tilde{\mathbf{u}}_2\|$. It can be easily proved that it is also one of the solutions of eq. (35) for $\lambda_1 = s\lambda_2$ if $\tilde{\mathbf{u}}_2 = \mu \tilde{\mathbf{u}}_1$:

$$\begin{aligned} s^2 \tilde{\mathbf{u}}_1^T \tilde{\mathbf{v}}_1 + s \tilde{\mathbf{u}}_1^T (\tilde{\mathbf{v}}_2 + \mu \tilde{\mathbf{v}}_1) + \mu \tilde{\mathbf{u}}_1^T \tilde{\mathbf{v}}_2 &= 0 \\ \Rightarrow (s + \mu) \tilde{\mathbf{u}}_1^T (s \tilde{\mathbf{v}}_1 + \tilde{\mathbf{v}}_2) &= 0. \end{aligned}$$

In the presence of noise, to avoid this solution for s resulting to $(\mathbf{0}_{4 \times 1}, \mathbf{q})$, we always choose from the two s -solutions the one that gives the largest value for $s^2 \tilde{\mathbf{u}}_1^T \tilde{\mathbf{u}}_1 + 2s \tilde{\mathbf{u}}_1^T \tilde{\mathbf{u}}_2 + \tilde{\mathbf{u}}_2^T \tilde{\mathbf{u}}_2$.

The sign variation in the solution for λ_2 in eq. (36) is due to the sign invariance of the solution: both $(\mathbf{q}^T, \mathbf{q}'^T)$ and $(-\mathbf{q}^T, -\mathbf{q}'^T)$ satisfy the motion equations and the constraints.

The computation algorithm consists of the following steps:

1. Given n motor motions $(\mathbf{b}_i, \mathbf{b}'_i)$ and the corresponding camera motions $(\mathbf{a}_i, \mathbf{a}'_i)$, check if the scalar parts are equal. Then extract the line directions and moments of the screw axes and construct the matrix T in eq. (33).
2. Compute the SVD of T and check if only two singular values are almost equal to zero (due to noise, we apply a threshold). Take the corresponding right-singular vectors $\tilde{\mathbf{v}}_7$ and $\tilde{\mathbf{v}}_8$.
3. Compute the coefficients of eq. (35) and solve it, finding two solutions for s .
4. For these two values of s , compute $s^2 \tilde{\mathbf{u}}_1^T \tilde{\mathbf{u}}_1 + 2s \tilde{\mathbf{u}}_1^T \tilde{\mathbf{u}}_2 + \tilde{\mathbf{u}}_2^T \tilde{\mathbf{u}}_2$, and choose the largest of them to compute λ_2 and then λ_1 .
5. The result is $\lambda_1 \tilde{\mathbf{v}}_7 + \lambda_2 \tilde{\mathbf{v}}_8$.

7. Experiments

To experimentally test the dual-quaternion method, we performed simulations and a real experiment. To compare its performance and experimentally substantiate the theoretical differences, we implemented two additional methods from the literature. The first one is similar to the method proposed by Horaud and Dornaika (1995), and is based (like ours) on the simultaneous computation of rotation and translation. Its representation consists of quaternions for the rotations and vectors for the translations. Equations (2) and (3) are combined additively into the following objective function:

$$J(\mathbf{q}, \tilde{\mathbf{t}}_X) = \|\mathbf{a}\mathbf{q} - \mathbf{q}\mathbf{b}\|^2 + \|((\mathbf{R}_A - \mathbf{I})\tilde{\mathbf{t}}_X + \tilde{\mathbf{t}}_A)\mathbf{q} - \mathbf{q}\tilde{\mathbf{t}}_B\|^2, \quad (37)$$

to be minimized with respect to \mathbf{q} and $\tilde{\mathbf{t}}_X$ subject to $\|\mathbf{q}\|^2 = 1$. After expressing the quaternion in spherical coordinates, we apply the Levenberg-Marquardt minimization in its NETLIB Fortran implementation. This method makes use of all of the information in the camera and motor motions, including the angles and the pitches, which are not used in the dual quaternion method. Like every iterative nonlinear minimization, it must be provided with starting values.

The second alternative method we applied was a two-step method as described by Chou and Kamel (1991). The first step solves for the rotation by minimizing

$$\|\mathbf{a}\mathbf{q} - \mathbf{q}\mathbf{b}\|^2 \quad \text{with respect to } \mathbf{q} \quad \text{subject to} \quad \|\mathbf{q}\|^2 = 1,$$

which can be reduced to an eigenvector problem. The second step solves the linear system of eq. (3) for the translation

$$(\mathbf{R}_A - \mathbf{I})\tilde{\mathbf{t}}_X = \mathbf{R}_X \tilde{\mathbf{t}}_B - \tilde{\mathbf{t}}_A.$$

In the following experiments and graphs, we denote our dual quaternion method by “DUAL,” the nonlinear simultaneous solution for rotation and translation by “NLIN,” and the separate solution by “SEPA.”

7.1. Synthetic Experiments

The intent of the synthetic experiments is to test the behavior of the above three methods under controllably varying factors. The simulation is conducted as follows: we establish N hand motions $(\mathbf{R}_B, \tilde{\mathbf{t}}_B)$ in a realistic setup similar to the real experiment of the next section. We add Gaussian noise of relative standard deviation of 1% corresponding to the angle readings. We assume a hand-eye setup and compute the camera motions $(\mathbf{R}_A, \tilde{\mathbf{t}}_A)$, to which we also add Gaussian noise of varying standard deviation, because this is the main source of error owing to the sensitive step of camera calibration. The noise is added as absolute value to the unit rotational quaternion, and as relative value to the translation. For every noise setting, each algorithm runs 1,000 times and outputs the estimated rotation quaternion $\hat{\mathbf{q}}$ and the estimated translation $\hat{\tilde{\mathbf{t}}}$ between the gripper and the camera. To qualify the results, we take the RMS of the errors in the rotation unit quaternion $\|\mathbf{q} - \hat{\mathbf{q}}\|$ and the RMS of the relative errors in the translation $\|\tilde{\mathbf{t}} - \hat{\tilde{\mathbf{t}}}\|/\|\tilde{\mathbf{t}}\|$. These are customary error metrics also used by Tsai and Lenz (1989) and Horaud and Dornaika (1995). However, the reader should be aware that the Frobenius norm of the difference of the rotation matrices $\|\mathbf{R} - \hat{\mathbf{R}}\|$ applied in these studies is much higher than the quaternionic error norm $\|\mathbf{q} - \hat{\mathbf{q}}\|$ ($2\sqrt{2}$ times larger if the axes are the same and the error is only in the angle).

In the first experiment, we tested a standard configuration of 20 hand motions under different noise levels in the camera poses. In Figure 3 we compare our algorithm (DUAL) with the nonlinear (NLIN) and the two-step (SEPA) algorithms. The dual-quaternion approach exhibits the best behavior, followed by the nonlinear minimizer. The reason for this discrepancy is the convergence of the nonlinear method to local minima in a subset of the 1,000 runs for each noise level, as well as the use of the angles and pitches in the nonlinear method.

In the second experiment, we keep the noise level at 1% and we vary the number of motions from 2 to 20. We observe (Fig. 4) the same behavior in the simultaneous and the separate solutions in the case of just two motions. This is plausible, since the number of unknowns is equal to the number of independent constraints in the pure rotational equations, making it irrelevant whether we solve separately or not. For a few motions, the nonlinear algorithm does not converge properly. The dual quaternion algorithm is superior in multiple motions.

In the third experiment, we varied the variance of the interstation rotation axes. According to work by Tsai and Lenz (1989), this is the most critical factor in the accuracy of hand-eye calibration. Again we keep the noise level at 1%, and choose 20 rotation axes from a varying area on the unit sphere characterized by the polar angle. The x -axis in the plot of Figure 5 represents the inverse of this area or the inverse of the axes' direction variance. The behavior is explained by Tsai and Lenz (1989) for the two-step separate solution algorithm

(SEPA): the smaller the variance in the direction of rotation axes, the higher is the estimation error. In the limiting case (not shown in the diagram) when all rotation axes are parallel the problem becomes singular. However, this is not an intrinsic property of the hand-eye calibration problem. We observe the striking phenomenon that the rotation error in both the nonlinear and the dual quaternion approaches is invariant to this variation. This is not a surprise, but is a main advantage of the approaches solving simultaneously for rotation and translation: rotation cannot be recovered from eq. (2) if all rotation axes are parallel. However, if both eq. (2) and eq. (3) are considered, a unique solution for rotation exists but the translation still possesses one degree of freedom (Chen 1991).

In all of the simulations, we observe the superior performance of the dual quaternion algorithm. The nonlinear minimizer could perform better if we could guarantee that it would converge to the global minimum, independent of the starting value. We experimentally showed that total ill-conditioning due to insufficient variation of the rotation axes is not an intrinsic property of the problem.

7.2. Real Experiments

The real experiments were conducted² with a Robosoft Pan-Tilt unit TO30 mounted on a controllable slider. The experimental configuration is illustrated in Figure 6. The axes of the camera coordinate system (x_c, y_c, z_c) are parallel to the axes (x_m, y_m, z_m) of the motor coordinate system. There is a relative translation between the two coordinate systems in the y - and z -directions. To avoid introducing new terms, in the following we refer to the motor coordinate system as the hand or the gripper.

Since the ground truth is unknown, we assess the performance of hand-eye calibration with two task-dependent methods. The first one—which is also applied in the classical paper by Tsai and Lenz (1989)—is the ability to predict the camera pose by using only the motor-motion data. This is very important for all tasks involving view planning or the opposite problem of gripper-pose planning. The second assessment is reconstruction by motion stereo using one camera: the camera is calibrated only once and then moved to new positions where it is not calibrated again, as would be the case in using a left-right camera stereo system.

In the first assessment, the camera was moved to 25 locations with different pan and tilt angles as well as different positions along the slider. The translation along the slider varied between 50 and 900 mm, and the calibration object was at an approximate distance of 1,000 mm. The camera was calibrated with the ellipse-based method (Tarel and Vzien 1996), which includes the computation of the 3×4 projective matrix

2. The image and motor recordings are courtesy of Jean-Philippe Tarel, SYN-TIM Project, INRIA Rocquencourt.

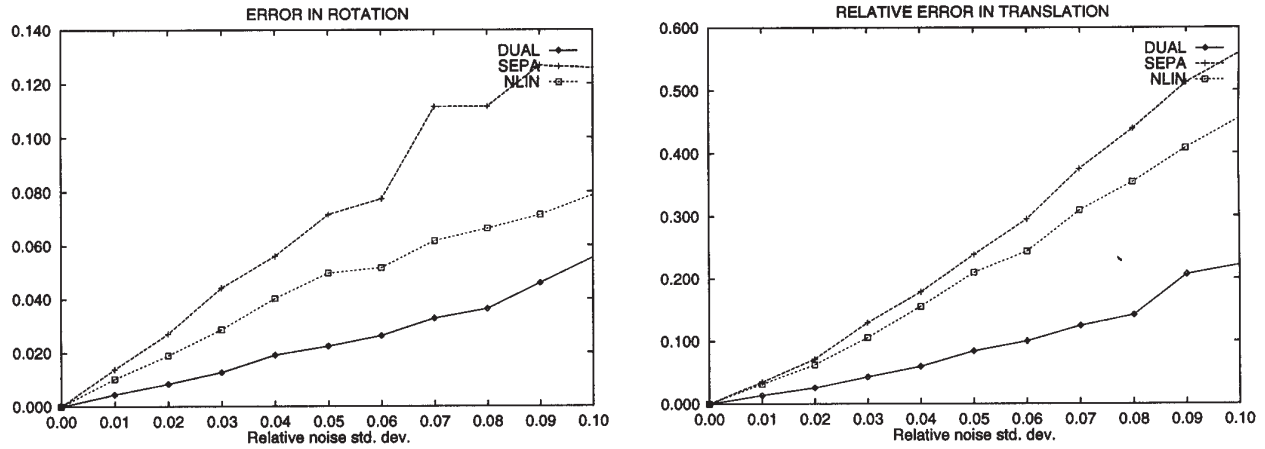


Fig. 3. Behavior of the dual quaternion (DUAL), the nonlinear (NLIN), and the two-step (SEPA) algorithms with variation in noise. The RMS rotation error is shown on the left; the RMS relative translation error is on the right.

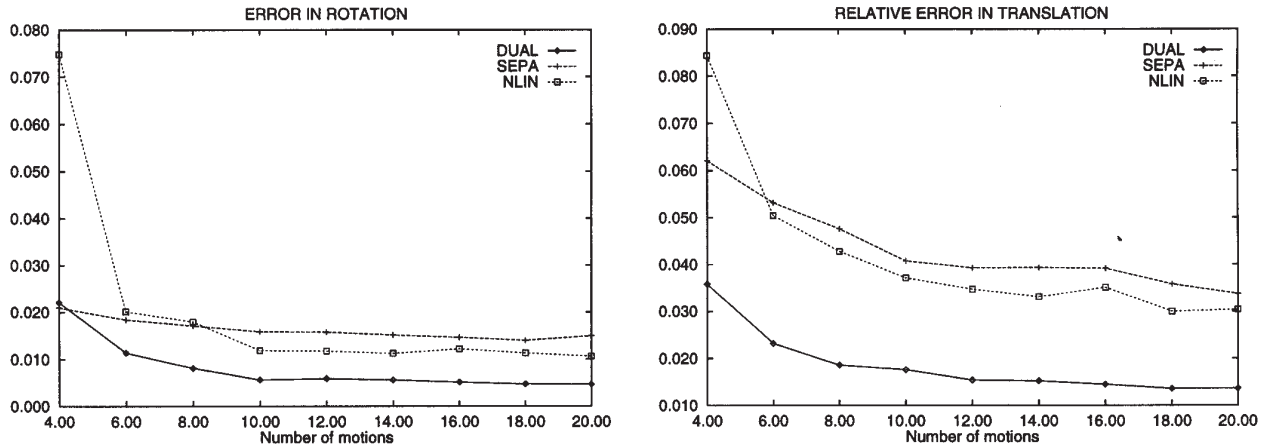


Fig. 4. The RMS error in rotation (left) and the RMS relative error in translation (right) as a function of the number of hand and camera motions.

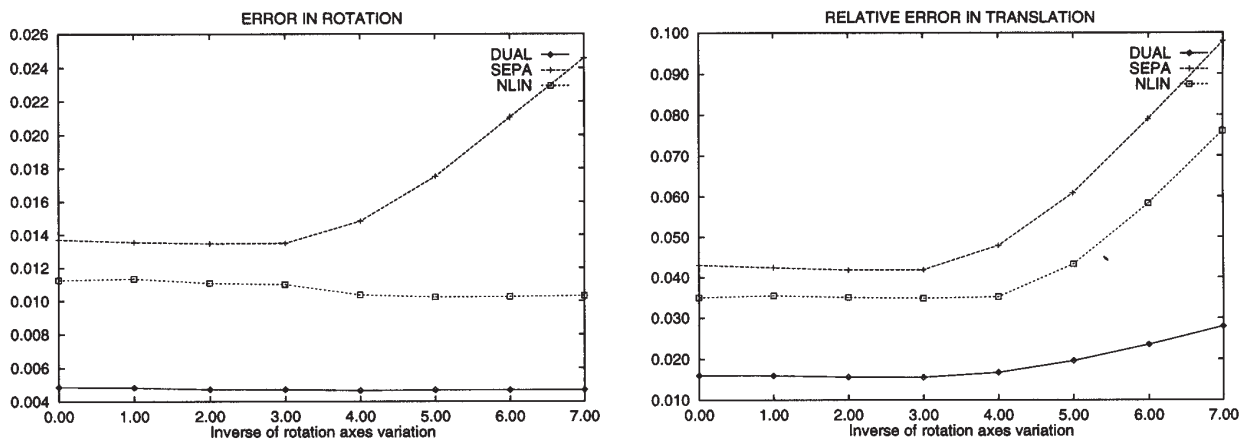


Fig. 5. The RMS error in rotation (left) and the RMS relative error in translation (right) as a function of the inverse of the rotation axes variation. The horizontal axis is proportional to the inverse of an area on the unit sphere inside where the rotation axes are distributed.

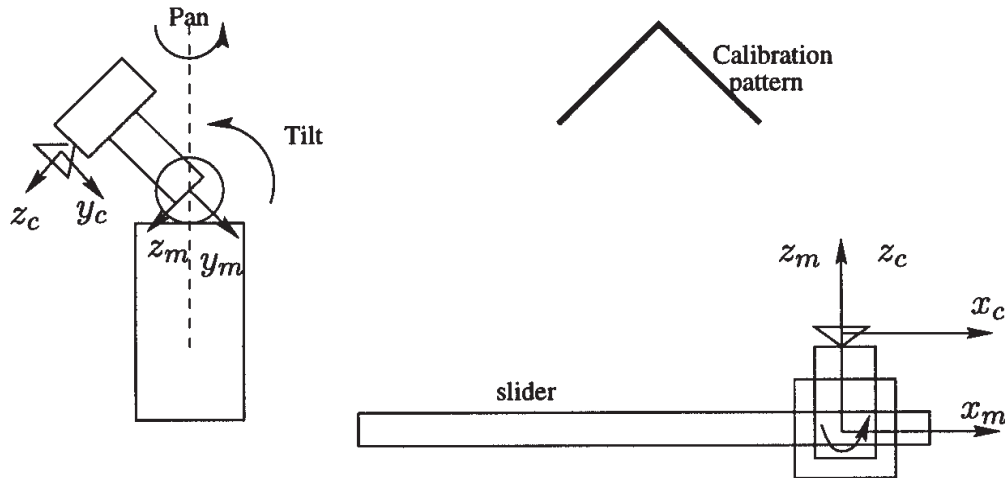


Fig. 6. The pan/tilt from a top view is shown on the left. The axes of the camera and the motor coordinate systems are parallel. The origins of the two coordinate systems differ by y - and z -offsets. On the right, we show the experimental setup with the slider, the pan/tilt head, and the calibration board.

as well as its decomposition in intrinsic and extrinsic parameters (Faugeras and Toscani 1986).

For $N = 11 \dots 19$ stations, we compute the hand-eye calibration by all three methods: the one proposed here using dual quaternions, the nonlinear simultaneous estimation, and the separate estimation of rotation and translation.

We extract the extrinsic parameters A_i from every projective camera matrix in eq. (4) and use them together with the motor poses B_i for the computation of the camera-gripper transformation X from N positions. Then we predict the camera pose for the verification stations $j = 20 \dots 25$ from the motor motion B_j and the first camera pose A_1 :

$$\hat{A}_j = X B_j^{-1} X^{-1} A_1.$$

We compare the predicted camera pose \hat{A}_j with the camera pose A_j extracted from the camera calibration, and average the errors over the five verification stations. The camera poses have an estimation error, but we assume that this is much lower than the error in the predicted pose. This procedure is repeated for a different number of frames $N = 10 \dots 20$ used in the computation of the hand-eye matrix X . The results for all three methods for varying N are shown in Figure 7, including the average absolute error for the rotation (left) and the average relative error for the translation (right). The number of verification stations was kept constant. The dual quaternion method was slightly superior. Both simultaneous methods (dual quaternion and nonlinear) performed better in the translation case, where all methods showed an error under 2%. We observed the expected decrease with the number of stations used; however, the decrease was not as steep as expected, because the variation in the interstation rotation axes was restricted (as explained in the next paragraph).

The error in the estimation of the hand-eye calibration depends on the errors in the camera poses and the motor recordings. Common sources of observed error in the assessment of all methods are in the extrinsic pose extraction for the verification stations and the motor recordings in moving to these stations. Translation computation is very sensitive to noise, due to the limited variation of the rotation axes of the interstation motions. This variation is constrained in that the calibration target must always be inside the field of view.

To obtain a rough perception of the values of the hand-eye transformation itself, the mapping computed with the dual quaternion methods using 20 stations was a rotation of 1.8° about the x -axis and a relative translation $(0, 125, -146)$ of the gripper with respect to the camera (cf. Fig. 6).

The second experiment, motion stereo, assesses the hand-eye calibration by one of each of the applications. Every time we have one camera and a controllable motion of a robot, we can produce a polynocular stereo configuration only if we know the actuator-to-camera transformation. It is also a direct assessment, since the assumed “ground truths” are the positions of the world points in space, which we know by designing the calibration object. In the first experiment, the “ground truth” was not veridical, since the poses computed after calibration and decomposition were erroneous. We show in Figure 8 two of the images used for the stereo reconstruction.

Stereo reconstruction with respect to a world-centered coordinate system necessitates the feature correspondences as well as two projective matrices, M_1 and M_2 , as defined in eq. (4) for two cameras. The correspondences are given because we used the same calibration pattern as an object to reconstruct. We applied all three methods described in the

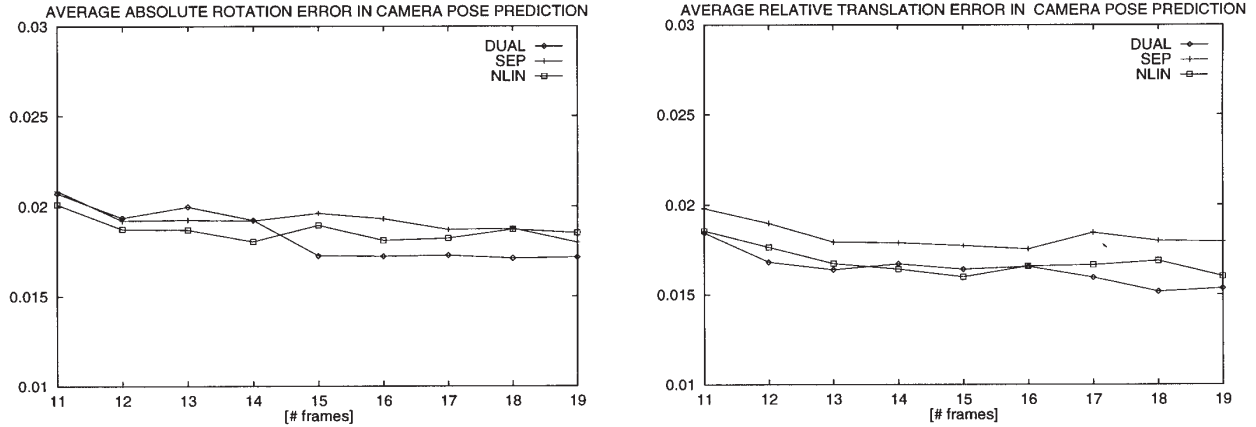


Fig. 7. The discrepancy between the predicted camera pose and the camera pose computed by camera calibration averaged over five verification stations. The absolute error for the rotation matrices is on the left, and the relative error in the translation vectors is on the right.

simulation section in two modes: the *extrinsic* mode and the *projective* mode.

In the extrinsic mode, we used the extrinsic camera poses to compute the interstation camera motions A , and the result was the camera-hand transformation X . Given only the first extrinsic matrix A_1 and the motor motion 1b_2 to a second position, the projection matrices could be computed only if the intrinsic parameter matrix C was known:

$$M_2 = C X {}^1b_2^{-1} X^{-1} A_1. \quad (38)$$

Given the correspondences in the first and the second images and the projection matrices M_1 from camera calibration and M_2 computed as above, we performed classical stereo triangulation.

The results of the extrinsic mode in all methods (denoted by DUAL, NLIN, and SEPA) are shown in the left side of Figure 9. In the same figure, we show the reconstruction (CAM) using the second projection matrix from calibration as if we were calibrating in every position. Of course, the latter is superior to all motion-stereo methods, because no errors from the motor encodings, the motor-angle offsets, or hand-eye calibration were involved. The same computed hand-eye transformation was used for all stations of the "second" camera. The curves show the absolute error for reconstruction between the 1st and the N th frame, where the baseline is increasing with N . We observed the reconstruction-error decay as the effective baseline increased. The nonregular behavior for specific stations was due to erroneous motor recordings.

In the projective mode, we avoided the decomposition in intrinsic and extrinsic parameters using the trick in eq. (5) (Horaud and Dornaika 1995). Equation (5) can be solved using dual quaternions in the same manner as in the first experiment. The result is the world-to-gripper transformation $Y = A_1^{-1} X$ at the first pose. The image-to-gripper

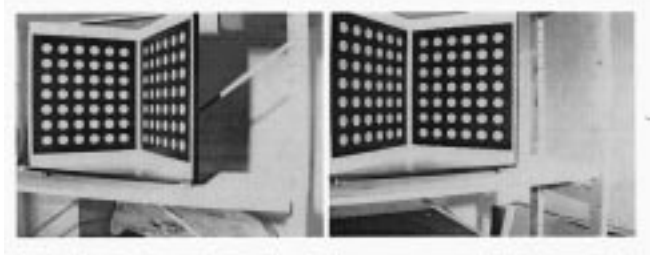


Fig. 8. The 1st (left) and the 22nd (right) image of the sequences of images used for stereo reconstruction.

transformation CX can be substituted by the image-to-world \times world-to-gripper transformation as $CX = M_1 Y$. The necessary second projection matrix reads as follows:

$$M_2 = M_1 Y {}^1b_2^{-1} Y^{-1}. \quad (39)$$

We observe that the second projection matrix can be written in terms of the solution of the hand-eye problem without decomposing any matrix in intrinsic and extrinsic parameters. The results are shown in the right side of Figure 9, and are in most of the cases about 25% better than the results in the extrinsic mode. This error reduction is due to a more-accurate hand-eye calibration using just projection matrices (eq. (6)) and owing to the fact that no decomposition was used in eq. (39) either. The outliers were observed in the same stations, which confirmed our conjectures that they arise due to motor-encoding errors in 1b_2 . In both modes we again observe the superiority of the methods solving simultaneously for rotation and translation.

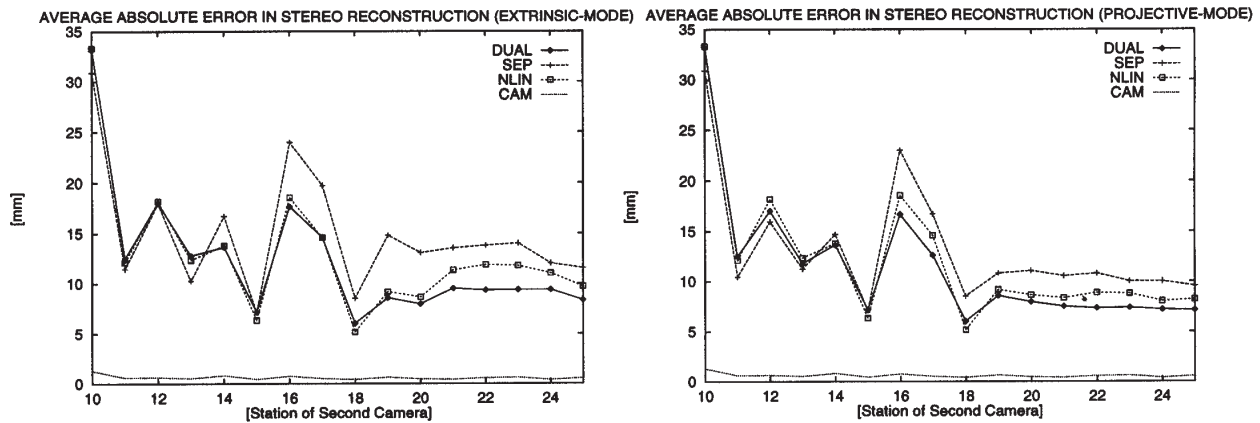


Fig. 9. The average reconstruction error in mm as a function of the station, which is proportional to the effective baseline (see also Fig. 6). The approximate depth of the points is about 100 mm. The lowest curve (CAM) shows the error for conventional reconstruction using projection matrices computed at every frame. The curves show the average error of reconstruction using the second projection matrix computed from the extrinsic mode (left) and the projective mode (right) of hand-eye calibration. We denote by DUAL, NLIN, and SEPA the dual-quaternion method, the nonlinear simultaneous method, and the separate solution, respectively.

8. Conclusion

Dual quaternions were long ago known in kinematics as the algebraic representation of screws. In this paper we introduced this language to formalize the screw approach to hand-eye calibration. We proved the fundamental fact that hand-eye calibration is a 3-D motion from the 3-D lines problem. The invariance of the angle and the pitch are straightforward results of the dual quaternion parameterization. This parameterization enabled us to establish a linear homogeneous system for the solution of all dual quaternion parameters. The computation of the null space with SVD and the consideration of the constraints for the dual quaternion to be unit yields a simple algorithm avoiding nonlinear steps.

We implemented two other methods, the first involving a nonlinear minimization but solving simultaneously for rotation and translation, and the second solving linearly first for the rotation and then for the translation. We compared all three methods in simulations where we varied the noise level in the camera and motor poses. We also tested the effect of the number of calibration stations as well as the effect of the main conditioning factor, which is the difference between the rotation axes' directions. The superiority of the dual quaternion method lies not only in the simultaneous solution for rotation and translation but also in the use of the information which is just necessary for the hand-eye calibration problem. The angle and the pitch of the camera and the motor screws are irrelevant to the problem, as also shown in the simulations. We applied all the methods in two variations in a real experiment of the active-vision area. To achieve a better assessment of the methods, we employed two different performance tests related to the tasks of controlled camera motion and stereo reconstruction,

respectively. We elaborate further on the dual quaternion approach for estimating hand-eye calibration in naturally singular configurations where conventional approaches are defeated. These include the calibration of cameras mounted on vehicles. Furthermore, the new representation opens new ways for the solution of many computer-vision problems involving line correspondences; for example, the extension of the algorithm presented here to the problem of registration of 3-D line sets is trivial.

Acknowledgments

Most of the work presented here was performed when the author was affiliated with the Cognitive Systems Group of the Kiel University. The author would like to thank Professor Hans-Hellmut Nagel for the common long discussions and calculations on dual numbers, as well as the comments made by Professor Thomas Beth five years ago; both paved the ground for the results obtained here. The author gratefully appreciates the constructive comments and advice of Professor Gerald Sommer, the careful reading and the hospitality of Professor Andre Galalowicz, and the discussions with Eduardo Bayro-Corrochano. The image and motor recordings in the first experiment are courtesy of Jean-Philippe Tarel, SYNTIM Project, INRIA Rocquencourt.

References

- Blaschke, W. 1960. *Kinematik und Quaternionen*. Berlin: VEB Deutscher Verlag der Wissenschaften.
- Chen, H. 1991 (June 3–6, Maui, HI). A screw-motion approach to uniqueness analysis of head-eye geometry. *Proc.*

- of the *IEEE Conf. on Comp. Vision and Pattern Recognition*. Los Alamitos, CA: IEEE, pp. 145–151.
- Chou, J., and Kamel, M. 1991. Finding the position and orientation of a sensor on a robot manipulator using quaternions. *Intl. J. Robot. Res.* 10(3):240–254.
- Clifford, W. 1873. Preliminary sketch of bi-quaternions. *Proc. London Math. Soc.* 4:381–395.
- Faugeras, O., and Toscani, G. 1986 (June 22–26, Miami Beach, FL). The calibration problem for stereo. *Proc. of the IEEE Conf. on Comp. Vision and Pattern Recognition*. Los Alamitos, CA: IEEE, pp. 15–20.
- Funda, J., and Paul, R. 1990. A computational analysis of screw transformations in robotics. *IEEE Trans. Robot. Automat.* 6:348–356.
- Gu, Y.-L., and Luh, J. 1987. Dual-number transformation and its application to robotics. *IEEE J. Robot. Automat.* 3:615–623.
- Horaud, R., and Dornaika, F. 1995. Hand-eye calibration. *Intl. J. Robot. Res.* 14:195–210.
- Li, M., and Betsis, D. 1995 (June 20–23, Boston, MA). Hand-eye calibration. *Proc. of the Intl. Conf. on Computer Vision*. Los Alamitos, CA: IEEE, pp. 40–46.
- Phong, T., Horaud, R., Yassine, A., and Pham, D. 1993 (May 11–14, Berlin). Optimal estimation of object pose from a single-perspective view. *Proc. of the Intl. Conf. on Comp. Vision*. Los Alamitos, CA: IEEE, pp. 534–539.
- Sabata, B., and Aggarwal, J. 1991. Estimation of motion from a pair of range images: A review. *CVGIP: Image Understanding* 54:309–324.
- Shiu, Y., and Ahmad, S. 1989. Calibration of wrist-mounted robotic sensors by solving homogeneous transform equations of the form $AX = XB$. *IEEE Trans. Robot. Automat.* 5:16–27.
- Study, E. 1891. Von den Bewegungen und Umlegungen. *Mathematische Annalen* 39:441–566.
- Tarel, J.-P., and Vzien, J.-M. 1996. *Camcal v1.0 Manual: A Complete Software Solution for Camera Calibration*. BTR, INRIA Rocquencourt.
- Tsai, R., and Lenz, R. 1989. A new technique for fully autonomous and efficient 3D robotics hand/eye calibration. *IEEE Trans. Robot. Automat.* 5:345–358.
- Walker, M. 1988. Manipulator kinematics and the epsilon algebra. *IEEE J. Robot. Automat.* 4:186–192.
- Walker, M., Shao, L., and Volz, R. 1991. Estimating 3-D location using dual number quaternions. *CVGIP: Image Understanding* 54:358–367.
- Wang, C. 1992. Extrinsic calibration of a vision sensor mounted on a robot. *IEEE Trans. Robot. Automat.* 8:161–175.